A model for surface EMG generation in volume conductors with spherical in-homogeneities

(Article begins on next page)

IEEE Transactions on Biomedical Engineering

A MODEL FOR SURFACE EMG GENERATION IN VOLUME CONDUCTORS WITH SPHERICAL INHOMOGENEITIES

Luca Mesin and Dario Farina

Laboratorio di Ingegneria del Sistema Neuromuscolare (LISiN), Dip. di Elettronica, Politecnico di Torino, Torino, Italy

Keywords: electromyography, modeling, tissue inhomogeneity, space invariance

Running title: Surface EMG and local tissue inhomogeneities

Corresponding author:

Dario Farina, PhD

Dipartimento di Elettronica, Politecnico di Torino; Corso Duca degli Abruzzi 24, Torino, 10129 ITALY

Tel. 0039-0114330476; Fax. 0039-0114330404; e-mail : dario.farina@polito.it

Acknowledgements

This work was supported by the European Shared Cost Project *Neuromuscular assessment in the Elderly Worker* (NEW) (QLRT-2000-00139), Fondazione “Cassa di Risparmio di Torino”, and Compagnia di San Paolo, Torino, Italy.

ABSTRACT

Most models for surface EMG signal generation are based on the assumption of space-invariance of the system in the direction of source propagation. This assumption implies the same shape of the potential distribution generated by a source in any location along the propagation direction. In practice, the surface EMG generation system is not space invariant, thus the surface signal detected along the direction of the muscle fibers may significantly change shape along the propagation path. An important class of non-space invariant systems is that of volume conductors in-homogeneous in the direction of source propagation. In this study we focused on inhomogeneities introduced by the presence of spheres of different conductivities with respect to the tissue where they are located. This may model the presence of glands, vessels, or local changes in the conductivity of a tissue. We present an approximate analytical solution that accounts for an arbitrary number of spheres in an arbitrary complex volume conductor. As a representative example, we propose the solution for a planar layered volume conductor, comprised of fat and muscle layers with spherical inhomogeneities inside the fat layer. The limitations of the approximations introduced are analytically discussed. The model is computationally fast and constitutes an advanced mean for the analysis and interpretation of surface EMG signal features.

1. INTRODUCTION

Many surface EMG models have been proposed in the past [28]. Their applications range from didactic purposes to the solution of a variety of research questions [5][8][19][31]. Most of the available surface EMG models are analytical, i.e., a mathematical explicit formula is provided as solution of the volume conduction problem. Numerical models have also been presented [18][26][10] and are necessary when dealing with complex geometries and/or conductivity tensors describing the volume conductor.

Analytical approaches have advantages over numerical ones and should be preferred when an analytical solution can be obtained [10]. Indeed, analytical solutions require less computational time than numerical ones, are exact (or the degree of approximation can be calculated), and allow to better relate the model parameters to the simulated signal. Thus, efforts towards the determination of analytical solutions for complex volume conductors are justified by the more flexible use of these types of solutions.

Most analytical models consider space invariant systems [2][4][7][9][13][20]. We defined as space invariance in the direction of propagation of the source (action potential) the property of a volume conductor of being both homogeneous and geometrically invariant along this direction [10]. This definition produces a class of volume conductors for which the simulation of surface detected EMG potentials can be viewed as a linear filtering problem. In particular, for space-invariant volume conductors, the potential distributions generated by two impulsive sources located at different positions along the direction of propagation are translated versions of each other, thus the response to a single source is sufficient to generate the potential as detected during source propagation. The space invariance property determines a significant simplification of the problem of simulating surface detected action potentials, as has been shown in previous model developments by applying properties of the 2-dimensional Fourier transform [7][9]. Since the space-invariance property is important to reduce the computational time also in case of numerical approaches (to avoid the computation of the source response for any location during propagation), numerical as well as analytical models are often limited to space invariant systems [18]. Non space-invariant systems may indeed lead to a non-acceptable computational time when investigated by a numerical method.

If a source moves at constant velocity along the space invariant direction and is detected along the same direction by different detection systems, the systems will record potentials with the same shape and a relative delay which depends on the distance between detection points. Thus, signal detection along a space invariant direction provides potentials of equal shape in any location. If the source changes during propagation, the surface detected potentials will also change depending on the detection point. The end-plate and end-of-fiber potentials, arising at the generation and extinction of the intracellular action potentials [14], originate from such changes in the source properties during propagation.

In the case of non-space invariant volume conductors, the potentials detected along the direction of propagation may have different shapes also without changes in the source properties. For non-space invariant systems, the response to an impulse may be different for any location of the impulse along the direction of propagation. In practical cases, modifications of the shape of the detected surface potentials when recorded at different locations along the direction of propagation are due to many factors, whose analytical description may be complex. Although limited attention has been devoted to the analytical analysis of systems non-space invariant in the direction of potential propagation, these systems constitute important models, with relevant practical applications.

An important class of non-space invariant systems is that of volume conductors in-homogeneous in the direction of source propagation. We recently investigated surface EMG generation from bi-pinnate muscles [21]. In this case, the inhomogeneity is due to the presence of two main fiber directions. In the present study we will focus on local inhomogeneities, i.e., spheres having conductivity different from that of the tissue in which they are located. We will present an analytical solution to this volume conduction problem, with approximations due to the complexity of the problem. The relative weight of the approximations introduced will be analytically investigated. The developed model will provide the means for generating action potentials detected from a volume conductor of any shape in which any number of local spherical inhomogeneities is introduced.

2. MODEL DEVELOPEMENT AND APPLICATIONS

We will begin with the case of infinite muscle tissue and we will then generalize to the case of any volume conductor. As an example of complex volume conductor, we will provide the solution for a two layer, planar medium with spherical inhomogeneities.

A. Mathematical problem for a volume conductor with a single inhomogeneity

In the case of quasi-stationary conditions, the electric potential in a volume conductor is obtained by the following relationship [3][15][22]:

$$\nabla \cdot J = -\nabla \cdot (\underline{\underline{\sigma}} \nabla \varphi) = I \qquad (1)$$

where φ is the electric potential, J is the current density in the medium (A/m^2), I is the source current density (A/m^3), and $\underline{\underline{\sigma}}$ the conductivity tensor (S/m).

A volume conductor with a localized inhomogeneity can be modeled by a discontinuous conductivity tensor:

$$\underline{\underline{\sigma}} = \underline{\underline{\sigma_c}}(1-\chi_p) + \sigma_p \chi_p \qquad (2)$$

where $\underline{\underline{\sigma_c}}$ is a continuous tensor, e.g., an anisotropic constant tensor modeling the muscle tissue, σ_p is the conductivity of the inhomogeneity, which will be assumed isotropic and constant, and χ_p is the characteristic function of the inhomogeneity. In particular:

$$\chi_p = \begin{cases} 1 & \Omega_p \\ 0 & \Omega \setminus \Omega_p \end{cases} \qquad (3)$$

where Ω is the domain considered and Ω_p the portion of the domain in which the inhomogeneity is defined (being $\Omega \setminus \Omega_p$ the notation chosen for the set difference between the domain Ω and the portion of the domain in which the inhomogeneity is defined Ω_p).

Considering $\Omega = \Re^3$, the mathematical problem of determining the potential due to an impulsive current δ in $\Omega \setminus \Omega_p$ can be stated as follows:

$$\begin{cases} -\nabla \cdot \left(\underline{\underline{\sigma_c}} \nabla \varphi_1 \right) = \delta & \Omega \setminus \Omega_p \\ -\nabla \cdot \left(\overline{\overline{\sigma_p}} \nabla \varphi_2 \right) = 0 & \Omega_p \end{cases} \tag{4}$$

with the condition of vanishing of the potential at infinity, and the following conditions of continuity of the potential and of the flux at the interface of the inhomogeneity:

$$\begin{cases} \varphi_1 = \varphi_2 & \partial\Omega_p \\ \underline{\underline{\sigma_c}} \dfrac{\partial \varphi_1}{\partial n} = \sigma_p \dfrac{\partial \varphi_2}{\partial n} & \partial\Omega_p \end{cases} \tag{5}$$

where *n* is the direction normal to the surface $\partial\Omega_p$ of the inhomogeneity. By linearity, the potential generated by any source current density is obtained by integrating over the domain Ω the impulsive response weighted by the source term. The problem described in Eqs. (4) and (5) is very complex, thus some simplifying assumptions on the geometry of the inhomogeneity are essential for an analytical treatment.

We will consider a spherical inhomogeneity. A closed solution can be obtained only in specific cases (such as with an inhomogeneity with infinite conductivity, [29]), using the image technique. Since we aim at providing a solution (even if approximated) which can be applied in more practical situations, we will need to exploit a more general approach.

The solution of the Laplace equation in spherical coordinates in azimuthal symmetry can be represented as [26]:

$$\varphi_{Sph}(r,\theta) = \sum_{n=0}^{n=+\infty} (A_n r^n + B_n r^{-(n+1)}) P_n(\cos\theta) \tag{6}$$

where P_n are the Legendre polynomials [1], and θ is the zenith angle. This expression, with proper choices of the coefficients A_n, B_n , can be used both to represent the solution in Ω_p and to study the effect of a spherical inhomogeneity on the potential distribution in $\Omega \setminus \Omega_p$ (in such a case, r measures the distance from the center of the inhomogeneity). Indeed, the solution in $\Omega \setminus \Omega_p$ is obtained, by linearity, from the summation of the solution associated to the impulsive source in absence of the inhomogeneity (i.e., for an infinite volume conductor, the impulse response is proportional to the inverse of the distance from the position of the source [23]), and the expression (6), in which r indicates the distance from the center of the inhomogeneity. As the terms in (6) with coefficient A_n diverge for $r \to \infty$, and those with coefficient B_n diverge for $r \to 0$, the A_n coefficients are null for the solution in $\Omega \setminus \Omega_p$, while the B_n coefficients vanish for the solution in Ω_p. We note that the solution in $\Omega \setminus \Omega_p$ can be interpreted as the sum of the inverse of the distance from the position of the source and a series of $\frac{1}{r}$, its gradient and all higher spatial derivatives, which are all solutions of the Laplace equation vanishing at infinity.

The solution to the problem can be obtained by imposing the interface conditions, matching all the terms of the series. An approximate solution is obtained considering only the first terms of the series in Eq. (6). This solution is valid for potentials observed at a certain distance from the inhomogeneity. Such an approximate solution and an estimate of the approximation error will be evaluated in the following.

B. Approximate solution

As the terms $\frac{1}{r^n}$ provide the largest contribution at a short distance from the inhomogeneity, an approximated solution can be obtained considering only some of these terms. The estimate of the error introduced in the solution can be expressed as function of the radius of the inhomogeneity, and the distances between the source, the inhomogeneity, and the detection point.

In this section we will consider the case of an inhomogeneity placed inside a homogeneous infinite ($\Omega = \Re^3$) isotropic volume conductor, i.e., $\underline{\underline{\sigma_c}} = \sigma$ in Eq. (2). The results apply also to the case of a homogeneous, anisotropic planar muscle, i.e., $\underline{\underline{\sigma_c}} = \sigma_t(\vec{i}\,\vec{i} + \vec{j}\vec{j}) + \sigma_l \vec{k}\vec{k}$, as it is possible to relate the problems of determining the impulse responses such an anisotropic planar volume conductor and of a isotropic one by the following change of the space variables, [15], [31]:

$$\begin{cases} X = \sqrt{\dfrac{\sigma}{\sigma_t}}x \\ Y = \sqrt{\dfrac{\sigma}{\sigma_t}}y \\ Z = \sqrt{\dfrac{\sigma}{\sigma_l}}z \end{cases} \tag{7}$$

It is worth noticing that, with such change of variables, the spherical inhomogeneity is transformed into an ellipse.

The problem may be solved by approximating the solution inside the inhomogeneity with a linear function. Such an approximation is justified as we assume the inhomogeneity to be small with respect to the distance from the source, so that it is reasonable to suppose the potential on $\partial\Omega_p$ to present small variations (yielding small variations inside the inhomogeneity, by the Mean Value Theorem for Laplace's equation). The perturbation of the potential in $\Omega \setminus \Omega_p$ due to the inhomogeneity is studied considering the following expression:

$$\varphi_p(\vec{r}\,) \approx \frac{a}{r} + \vec{A} \cdot \nabla \frac{1}{r} = \frac{a}{r} - \frac{\vec{A} \cdot \vec{n}}{r^2} \tag{8}$$

(a and $\vec{A}$ being a scalar and a vector to be determined) which is a harmonic perturbation (i.e., a term satisfying Eq. (4)) of the inhomogeneity free potential, i.e., the potential corresponding to the case of the homogeneous volume conductor obtained by removing the inhomogeneity. The expression (8) approximates the perturbation effect of the inhomogeneity considering only the first two non vanishing terms in the series (6). As the first term in the right hand side of Eq. (8) would give a flux proportional to a through a closed surface surrounding the inhomogeneity, we set $a = 0$ [16]. Thus, the approximate solution to Eq. (4) in $\Omega \backslash \Omega_p$ can be written as the sum of the inhomogeneity free solution and the perturbation term (Figure 1):

$$\varphi_1(\vec{r}\,) = \varphi_s(\vec{r}\,) + \varphi_p(\vec{r}\,) \approx \frac{1}{|\vec{r} - \vec{r}_s|} - \frac{\vec{A} \cdot \vec{n}}{|\vec{r} - \vec{r}_p|^2} \qquad (9)$$

where $\vec{r}_s$ is the position of the source and $\vec{r}_p$ indicates the position of the center of the inhomogeneity (Figure 1).

Figure 1 about here

The boundary conditions at the surface of the spherical inhomogeneity impose a correction to the potential $\frac{1}{|\vec{r} - \vec{r}_s|}$. Such a correction is larger in the direction joining the center of the sphere to the source position ($\frac{\partial \varphi_1}{\partial n}$ is maximum), and decreases considering the orthogonal directions ($\frac{\partial \varphi_1}{\partial n}$ vanishes in a circumference laying in the plane orthogonal to $\vec{r}_s - \vec{r}_p$; the points of such a circumference are obtained as tangent points of the sphere to the straight lines through $\vec{r}_s$) (Figure 2). Thus $\vec{A}$ should be chosen in the direction parallel to $\vec{r}_s - \vec{r}_p$.

Figure 2 about here

The magnitude of $\vec{A}$ can be determined studying a one dimensional problem along the direction of $\vec{A}$. We will indicate by s the arc length along such a direction. Imposing the boundary conditions at the surface of the sphere, i.e., at $s_p - R$ and $s_p + R$ (where R is the radius of the inhomogeneity and s_p its center), we obtain (Figure 1):

$$
\begin{cases}
\left.\dfrac{1}{s-s_s}\right|_{s_p-R} - \left.\dfrac{\vec{A}\cdot(-\vec{i}\,)}{(s-s_p)^2}\right|_{s_p-R} = \varphi_2(s_p-R) \\
\left.\dfrac{1}{s-s_s}\right|_{s_p+R} - \left.\dfrac{\vec{A}\cdot\vec{i}}{(s-s_p)^2}\right|_{s_p+R} = \varphi_2(s_p+R) \\
\left.\sigma\dfrac{\partial}{\partial s}\dfrac{1}{s-s_s}\right|_{s_p-R} - \left.\sigma\dfrac{\partial}{\partial s}\dfrac{\vec{A}\cdot(-\vec{i}\,)}{(s-s_p)^2}\right|_{s_p-R} = -\sigma_p\dfrac{\Delta\varphi}{2R} \\
\left.\sigma\dfrac{\partial}{\partial s}\dfrac{1}{s-s_s}\right|_{s_p+R} - \left.\sigma\dfrac{\partial}{\partial s}\dfrac{\vec{A}\cdot\vec{i}}{(s-s_p)^2}\right|_{s_p+R} = -\sigma_p\dfrac{\Delta\varphi}{2R}
\end{cases}
\qquad (10)
$$

where we assumed $s_p > s_s > 0$, $\vec{i}$ is the unit vector along the direction of the positive *s*-axis, $\Delta\varphi = \varphi_2(s_p-R) - \varphi_2(s_p+R)$. Note that in the third and fourth conditions, which are those concerning the continuity of the flux, φ_2 is assumed a linear function of *s*. With further algebraic calculations (omitted) and using a linear approximation of $\dfrac{1}{s-s_s}$ in (s_p-R, s_p+R), we obtain the following solution:

$$
\begin{aligned}
\Delta\varphi &= \frac{6\sigma}{2\sigma+\sigma_p}\frac{R}{(s_p-s_s)^2} \\
\vec{A}\cdot\vec{i} &= \frac{\sigma-\sigma_p}{2\sigma+\sigma_p}\frac{R^3}{(s_p-s_s)^2}
\end{aligned}
\qquad (11)
$$

We note that the correction term vanishes if $\sigma = \sigma_p$. Considering the limit case for which the inhomogeneity is modeled as a perfect conductor ($\sigma_p = \infty$), the solution provided is the first order approximation of the exact solution [29], obtained by the image theory for the potential generated by a point source in a homogeneous infinite volume conductor with a sphere of infinite conductivity at a potential equal to the one that would be in the same volume without the in-homogeneous sphere at its center (equal to the average of the potential over the sphere or over its surface by the Mean Value Theorem for Laplace’s equation). In such a case we also obtain $\Delta\varphi = 0$, as expected. Another limit case is that of a sphere of insulating material. In this case, the solution is an approximation of a Neumann homogeneous problem, for which the solution has vanishing normal derivative on the inhomogeneity surface. The approximated solution provided imposes the vanishing of the normal derivative along $\vec{r}_s - \vec{r}_p$, which is the steepest descent direction of the potential, and in the orthogonal section through the center of the inhomogeneity.

Figure 3 shows the potentials in the free space (in the direction $\vec{r}_s - \vec{r}_p$) with inhomogeneities of different conductivities. In the case $\sigma_p = 0$, the normal derivative on the inhomogeneity boundary is very small (it should vanish). For the case $\sigma_p = +\infty$, the difference between the potentials on the boundary points is very small (it should vanish). It is worth noting the different effects in the cases in which the ratio $\frac{\sigma_p}{\sigma}$ is larger or smaller than 1.

Figure 3 about here

C. Analysis of the errors in the approximation

The approximate solution provided above is a first order approximation. As noted previously, the effect of the inhomogeneity is larger in the direction of $\vec{A}$. We can estimate the error in such a direction by considering other terms in the series expansion. Studying an approximation of the third order for $\frac{1}{r}$, and adding correction terms $\delta\varphi_1, \delta\varphi_2$ (on the left and on the right of the inhomogeneity center, respectively) for the potential variation:

$$\Delta\varphi' = \Delta\varphi + \delta\varphi_1 + \delta\varphi_2 \qquad (12)$$

where:

$$\varphi_2(s_p - R) \approx \varphi_2(s_p) + \frac{\Delta\varphi}{2} + \delta\varphi_1, \varphi_2(s_p + R) \approx \varphi_2(s_p) - \frac{\Delta\varphi}{2} + \delta\varphi_2 \qquad (13)$$

and for the normal derivatives of the potential internal to the inhomogeneity:

$$\left.\frac{\partial\varphi}{\partial n}\right|_{s_p-R} \approx \frac{\Delta\varphi}{2R}+\frac{\delta\varphi_1}{R},$$
$$\left.\frac{\partial\varphi}{\partial n}\right|_{s_p+R} \approx \frac{\Delta\varphi}{2R}+\frac{\delta\varphi_2}{R} \tag{14}$$

we obtain the following approximated expression for the potential outside the inhomogeneity:

$$\varphi(s)=\frac{1}{s-s_s}+\varphi_p(s)\approx\frac{1}{s-s_s}-\frac{\vec{A}\cdot\vec{n}}{(s-s_p)^2}-\frac{\beta}{(s-s_p)^3} \tag{15}$$

Calculations omitted yield to $\beta \propto \frac{R^6}{\left(s_p-s_s\right)^4}$, with a proportionality constant (which depends on the conductivities of the volume conductor and of the inhomogeneity) smaller than one. If the minimum distances between the source, the center of the inhomogeneity, and the detection point are larger than kR ($k \in \Re$), the ratio between the term $\frac{\beta}{(s-s_p)^3}$ (omitted in the approximate solution in the previous section) and the free space potential $\frac{1}{s-s_s}$ is less than $\frac{1}{k^6}$, which is an estimate of the importance of the higher order correction terms over the total potential; the ratio between $\frac{\vec{A}\cdot\vec{n}}{(s-s_p)^2}$ and $\frac{\beta}{(s-s_p)^3}$ is less than $\frac{1}{k^3}$, which is an estimate of the effect of the correction term only on the perturbation induced by the inhomogeneity. Considering terms of higher order, the new contributions will give, in the worst case, an effect of the order $\frac{1}{k^{3n}}$ on the simulated potential. This computation of the error in the approximation allows to select the minimum distance between the source and the inhomogeneity in order to maintain the error small enough.

A further analysis necessary to investigate the errors due to the approximations introduced concerns the solution in the direction normal to the vector $\vec{A}$. As noted above, the normal derivative of the free space solution vanishes along a circumference belonging to the boundary of the inhomogeneity in a plane normal to $\vec{A}$. The perturbation term should vanish along that circumference. However, the approximated perturbation term $\frac{\vec{A}\cdot\vec{n}}{(s-s_p)^2}$ vanishes in the plane normal to $\vec{A}$, passing through the center of the sphere. The distance between the parallel planes containing the two circumferences is (Figure 2):

$$d = \frac{R^2}{\left|\vec{r}_s - \vec{r}_p\right|}, \qquad (16)$$

The circumference associated to the exact solution is closer to the source (Figure 2). We can consider d as a measure of the asymmetry of the perturbation term in the angular direction. We could correct it by shifting the discontinuity of the approximate perturbation term $\frac{\vec{A}\cdot\vec{n}}{(s-s_p)^2}$ toward the source (with a trade-off between compensating the angular error and maintaining a good approximation in the direction of $\vec{A}$, which is the most important term far from the inhomogeneity) or using a higher order term. Both these procedures yield to terms which vanish rapidly far from the inhomogeneity.

In the representative results presented we will consider conditions in which the distances between the source, the inhomogeneity, and the detection point are always sufficiently large to have the worst case error smaller than 10% of the perturbation term. The worst case condition corresponds to the source located at the minimum distance from the inhomogeneity, with the source, the inhomogeneity and the detection point located on the same line. This condition may be verified only for a specific time instant. In all other cases the error is smaller than the worst case one.

D. Including more than one spherical inhomogeneity

When more than one sphere is considered, by linearity we could sum the perturbation terms corresponding to each sphere. However, the perturbation term due to a sphere, as evaluated at the location of another inhomogeneity, may be comparable to the free space potential evaluated at such a position. In this case, the perturbation term of the inhomogeneity considered should take into account the sum of the total potential produced by the source and the first inhomogeneity. This generates mutual terms in the expression of the approximated potential, considerably increasing the complexity of the solution.

If the source and the inhomogeneities are not placed along the same line (which is never the case, apart possibly one time instant, as we are interested in moving sources), the one dimensional analysis performed in the previous sections can not be applied. Nevertheless, as the perturbation term is largest along the line between the source and the center of the inhomogeneity, studying the case in which the source and the inhomogeneities are aligned provides an estimate of the mutual effect of the inhomogeneities in the worst case. As we are interested in localized inhomogeneities, we will not consider the mutual effect but rather we will choose a distance between inhomogeneities which guarantees a negligible worst case mutual effect. For this purpose, the perturbation introduced by an inhomogeneity on a second one should be analyzed.

The effect of the perturbation term associated to an inhomogeneity on another inhomogeneity can be studied comparing the free space potential on the second inhomogeneity ($\frac{1}{\left|\vec{r}_{p2} - \vec{r}_s\right|}$) with the perturbation term relative to the first inhomogeneity on the second one ($\frac{\vec{A}\cdot\vec{n}}{\left|\vec{r}_{p1} - \vec{r}_{p2}\right|^2}$,where *p1, p2* refer to the two inhomogeneities). Imposing the perturbation term at least *k* times smaller than the free space term, a sufficient condition (i.e., a worst case condition) is (Figure 4):

$$k\frac{\alpha^2}{\rho^2 d_{12}^2} < \frac{1}{r} \quad \rightarrow \quad d_{12} > \alpha\frac{\sqrt{kr}}{\rho} \tag{17}$$

where the terms have been normalized with respect to the inhomogeneity radius *R*, d_{12} being the normalized distance between the centers of the inhomogeneities, ρ the normalized distance between the source and the first inhomogeneity, r the normalized distance between the source and the second inhomogeneity, and $\alpha = \sqrt{\frac{\sigma - \sigma_p}{2\sigma + \sigma_p}} < 1$. The source and the inhomogeneities have been considered aligned (worst case because the effect of the inhomogeneity is the largest, and because in Eq. (17) the alignment implies that $d_{12} = r - \rho$, which is the minimum value of d_{12} for fixed r and ρ, as shown in Figure 4). Substituting $r = d_{12} + \rho$ in Eq. (17), we obtain d_{12} as a function of the distance from the source to the first inhomogeneity ρ:

$$d_{12} > \frac{\alpha^2 k + \sqrt{\alpha^4 k^2 + 4\alpha^2 k \rho^3}}{2\rho^2} \tag{18}$$

It is worth noting that a two inhomogeneities model should be considered even in the case of a single inhomogeneity in the volume conductor, when we are interested in a homogeneous Neumann problem (insulated volume conductor), whose solution requires the application of the image theorem (Figure 4). Thus, Eq. (17) imposes a minimal depth of the inhomogeneity as a function of the fiber depth in the volume conductor.

Figure 4 about here

E. General Volume Conductors

The approach introduced in the previous sections for one layer volume conductor can be generalized to more complex conductors. The effect of a spherical inhomogeneity can be approximated by adding a perturbation term involving the gradient of $\frac{1}{r}$. In the general case, an explicit analytical solution of the in-homogeenity free potential may not be available. However, for solving the problem it is sufficient to calculate the inhomogeneity free solution (analytically or numerically) on the boundary of the inhomogeneity. For a best fit of the effect of the inhomogeneity, the approximate perturbation term should be maximum in the direction of the largest rate of variation of the inhomogeneity free solution, i.e., in the direction of its gradient. Thus, at a first order approximation, the gradient of the inhomogeneity free solution in the center of the inhomogeneity is sufficient to study the approximated perturbation effect of the inhomogeneity.

Following the same steps as above and assuming known the gradient of the impulsive response of the volume conductor, the following system of equation is obtained at a first order approximation:

$$\begin{cases} 2R|\nabla\varphi| + 2\dfrac{\vec{A}\cdot\vec{n}}{R^2} = \Delta\varphi \\ -2\sigma|\nabla\varphi| + 4\sigma\dfrac{\vec{A}\cdot\vec{n}}{R^3} = -\sigma_p\dfrac{\Delta\varphi}{R} \end{cases} \qquad (19)$$

with the same notations as before [Eq. (10)] and the potential variation $\Delta\varphi$ evaluated along the direction of the gradient of the potential. The solution is given by:

$$\begin{aligned} \Delta\varphi &= \frac{6\sigma}{2\sigma+\sigma_p}|\nabla\varphi|R \\ \vec{A}\cdot\vec{n} &= \frac{\sigma-\sigma_p}{2\sigma+\sigma_p}|\nabla\varphi|R^3 \end{aligned} \qquad (20)$$

When a homogeneous Neumann condition at the surface of the volume conductor is considered, it is needed to study the effect of the perturbation term on such a surface. Indeed, the inhomogeneity provides a contribution with a normal derivative to the surface which has to be annihilated, by linearity, by adding a further term located out of the domain. In the case of planar volume conductors [7], it is necessary to place another identical sphere at the symmetric point with respect to the planar surface (image theorem, Figure 4).

F. Example of application: two-layer planar volume conductor

The problem of surface EMG simulation in the case of a multi-layer planar volume conductor was investigated in [7]. Using the same approach, the following transfer function for a two layer planar volume conductor (Figure 5) is obtained (calculations omitted):

$$H(k_x, y, k_z) = \frac{1}{2\sigma_{MT}} \frac{e^{-\sqrt{k_x{}^2+\frac{\sigma_{ML}}{\sigma_{MT}}k_z{}^2}|y_0|}}{\cosh(k_y h)\left(\sqrt{k_x{}^2+\dfrac{\sigma_{ML}}{\sigma_{MT}}k_z{}^2}+k_y\dfrac{\sigma}{\sigma_{MT}}\tanh(k_y h)\right)}\left(e^{k_y(y-h)}+e^{-k_y(y-h)}\right), \quad y\in[0,h]$$

(21)

where $\sigma, \sigma_{ML}, \sigma_{MT}$ are the conductivities of the fat layer, and of the muscle in the directions longitudinal and transversal to the fibers, respectively, $k_y = \sqrt{k_x^2 + k_z^2}$ (k_x and k_z being the spatial angular frequencies in x and z directions, respectively), the depth is measured by the y coordinate, y_0 is the source depth (<0), $y = 0$ is the position of the interface between fat and muscle, $y = h$ is the detection surface.

In [7] the transfer function was provided only for the detection surface while the expression (21) refers to a generic depth y into the fat layer, which is here of interest to study the effect of the inhomogeneity. We will consider spherical inhomogeneities placed in the fat layer. Generalizations of this case to multi-layer planar volume conductors are straightforward.

The gradient of the inhomogeneity free potential at the center of the inhomogeneity is given by:

$$\nabla \varphi = \begin{pmatrix} \Im_2^{-1}\left(jk_x H\right) \\ \Im_2^{-1}\left(\partial_y H\right) \\ \Im_2^{-1}\left(jk_z H\right) \end{pmatrix} \tag{22}$$

where $\Im_2^{-1}$ is the two-dimensional inverse Fourier transform in k_x, k_z and H is given by Eq. (21). Note that the partial derivatives in the x and z coordinates are obtained in the spatial frequency domain, which is also the domain in which the problem has been studied [Eq. (21)] [7]. Substituting the expression (22) in (20), the perturbation term is obtained by Eq. (8). The surface potential is obtained summing the inhomogeneity free potential and the perturbation term at the detection surface:

$$\varphi\ (x, y = h, z) = \varphi_s(x, y = h, z) + \varphi_p(x, y = h, z) \approx \Im_2^{-1}(H(k_x, y = h, k_z)) - \left.\frac{\vec{A} \cdot \vec{n}}{\left|\vec{r} - \vec{r}_p\right|^2}\right|_{y=h} \tag{23}$$

For the numerical issues related to the inversion of the transfer function, i.e., a proper choice of the sampling in the spatial frequency domain, we refer to [7]. The numerical errors in the inverse Fourier transformation can be studied by comparison with the one layer solution, for which an analytical approximate solution is known in the space domain.

Figure 5 about here

G. Representative Simulations

Figure 6 reports examples of surface EMG signals filtered by spatial filters usually applied for EMG detection in the case of absence and presence of a local inhomogeneity. A small displacement of the inhomogeneity from the aligned (with the source and the electrode) situation is also considered. The figure shows that different spatial filters may have different sensitivities to local inhomogeneities. The sensitivity depends on the relative location of the inhomogeneities with respect to the electrodes forming the spatial filter, thus the results may be largely different for other geometrical arrangements with respect to those of Figure 6.

Figure 6 about here

3. DISCUSSION AND CONCLUSION

In this study we proposed the analytical solution of the problem of surface EMG signal generation in volume conductors with spherical inhomogeneities. The presence of local inhomogeneities complicates significantly the analytical problem with respect to the analysis of the correspondent systems without the inhomogeneities.

The systems analysed in this work are non-space invariant in the direction of source propagation, which makes the potential distribution different in shape for any location of the source along the propagation path. In the literature, only a few systems of this type have been investigated [21][26], either numerically or analytically. The availability of models of non-space invariant systems is relevant for the analysis of methods of signal detection or processing which are theoretically based on the absence of shape changes of the detected potentials along the direction of propagation. In practice, this condition is not met, thus the performance is affected by the mismatch between the hypotheses on which the techniques are designed and the practical situation.

A relevant example of techniques theoretically based on the pure propagation of the signal is spatial filtering. The classic bipolar recording is the simplest example of spatial filter and can be described by an analytical spatial transfer function, derived from the assumption of signal propagation along the direction of the fibers [17]. The same applies for other one- or two-dimensional spatial filters [24][25]. The comparison of filter selectivity is based on the high-pass frequency [6]; the higher the cut-off frequency, and the steeper the transfer function, the higher the selectivity of the filter. However, the transfer functions derived in the literature can not be applied in case of non-space invariant systems. In this case the deviation of performance of the filter applied for signal detection can only be investigated by models describing non-space invariant systems.

Similarly, the methods developed for the estimation of muscle fiber conduction velocity are based on the assumption that the detected potentials are identical in shape and delayed [12]. The delay is related to the velocity of propagation. If the detected potentials do not have the same shape, there is not a unique definition of delay, thus different methods for its estimation may provide significantly different results. Moreover, some methods may be more or less sensitive to the shape variations, and thus can be preferred over others after an evaluation of performance based on models describing non-space invariant systems.

Although the complexity of the analytical solution can be avoided by a numerical approach, an analytical solution is important for many reasons, such as the low computational time. Moreover, the analytical investigation allows a better insight into the physical phenomena which underlie the modifications in the signal characteristics, providing a detailed analysis of the generation of the potential distribution. For example, this study shows that the perturbation effect tends to zero as the inverse of the square of the distance from the detection point and the support of the perturbation on the detected signal travels in opposite direction with respect to the propagating source (see Figure

1.a). The latter observation indicates that this kind of inhomogeneities may have a large effect on conduction velocity estimation.

In conclusion, this study provides an analytical approximation of the potential distribution in complex in-homogeneous volume conductors and, also because of the low computational time, constitutes the means for systematically analysing methods for surface EMG processing in conditions closer to the practical situation. Such means were not previously available and allow the development and characterisation of new methods for information extraction.

Approximations and limitations of the approach

The limitations of the proposed model are due to the approximation introduced, explained through the paper. The approximations are mainly due to the truncation of series (6) and to neglecting the mutual effects between inhomogeneities. The first approximation can be removed by considering a more precise approximation by the same technique adding more terms in the series expansion approximating the solution (8). In this way, near field effects could be considered, widening the application of the method, adapting the method to the specific condition. To enlarge the minimal distance between the inhomogeneities is not simple, as mutual effects are difficult to handle analytically; a new model should be studied. This is an intrinsic characteristic of the topic addressed, as we are focused on local inhomogeneities: adding more inhomogeneities close to each other is the basis for the development of a model of a distributed inhomogeneity, which is out of the purposes of the paper.

The main limitations of the method, as it is presented in the paper (without introducing more detailed approximations), concern the relation between the dimension of the inhomogeneities, their position with respect to the source and to each other (Eq. (18)). Note that in a recent application of this model [11] we proved that the perturbation effect due to local inhomogeneities (as modeled in the present manuscript) is very relevant on estimates of conduction velocity. A plane layer model with 3 inhomogeneities into the fat layer (4 mm thick) and fiber 4 mm deep in the muscle was used.

In all the simulations the worst case approximation error was smaller than 5% of the perturbation term (distance between two spheres larger than $3 \cdot R$, all the inhomogeneities depths equal to $2 \cdot R$, where R=1 mm is the radius of the three inhomogeneities considered for each of the simulations).

Interesting simulations of physiological relevance can then be obtained by the proposed method. More situations can be described by adapting the method to a more precise simulation (as precise as required, by adding more and more terms of the series (6), being careful to the computational cost, which is slightly increasing by adding terms to the approximated solution). Finally, further developments are suggested to account for a distributed inhomogeneity, not taken into account in this paper.

References

1. M. Abramowitz, I.A. Stegun, *Handbook of mathematical functions*, New York: Dover, 1965
2. J.H. Blok, D.F. Stegeman, and A. van Oosterom, “Three-layer volume conductor model and software package for applications in surface electromyography,” *Ann. Biomed. Eng.*, vol. 30, pp. 566-77, 2002.
3. J. Clark, R. Plonsey, “The extracellular potential field of the single active nerve fiber in a volume conductor”, *Biophys. Journ*., vol. 8, pp. 842-64, 1968
4. G.V. Dimitrov, N.A. Dimitrova. “Precise and fast calculation of the motor unit potentials detected by a point and rectangular plate electrode”, *Med Eng Phys*., vol. 20, pp 374-81, 1998.
5. N.A. Dimitrova, G.V. Dimitrov. “Amplitude-related characteristics of motor unit and M-wave potentials during fatigue. A simulation study using literature data on intracellular potential changes found in vitro”, *J Electromyogr Kinesiol*, vol. 12, pp. 339-49, 2002.
6. C. Disselhorst-Klug, J. Silny, G. Rau, “Improvement of spatial resolution in surface-EMG: a theoretical and experimental comparison of different spatial filters”, *IEEE Trans. Biomed. Eng.*, vol. 44, pp. 567 – 574, 1997.
7. D. Farina, R. Merletti, “A novel approach for precise simulation of the EMG signal detected by surface electrodes”, *IEEE Trans. Biomed. Eng.*, vol. 48, pp. 637-646, 2001
8. D. Farina, C. Cescon, R. Merletti, “Influence of anatomical, physical, and detection-system parameters on surface EMG” *Biol Cybern.*, vol. 86, pp. 445-56, 2002
9. D. Farina, L. Mesin, S. Martina, R. Merletti, “A surface EMG generation model with multi-layer cylindrical description of the volume conductor”, *IEEE Trans. Biomed. Eng.,* vol. 51, pp. 415-426, 2004
10. D. Farina, L. Mesin, S. Martina, “Advances in surface electromyographic signal simulation with analytical and numerical descriptions of the volume conductor”, *Med. Biol. Eng. Comput.*, in press

11. *Sensitivity of surface emg-based conduction velocity estimates to local tissue inhomogeneities – influence of the number of channels and inter-channel distance*, *Journal of Neuroscience Methods,* in press (2004); available on line)
12. D. Farina, R. Merletti, "Methods for estimating muscle fiber conduction velocity from surface electromyographic signals", Med. Biol. Eng. Comput., in press
13. T.H. Gootzen, D.F. Stegeman, A. Van Oosterom, "Finite limb dimensions and finite muscle length in a model for the generation of electromyographic signals", *Electroencephalogr Clin Neurophysiol.* vol. 81, pp. 152-62, 1991
14. A. Gydikov, L. Gerilovski, N. Radicheva, N. Troyanova "Influence of the muscle fiber end geometry on the extracellular potentials", *Biol Cybern*, vol. 54, pp. 1-8,1986
15. A. Heringa, D.F. Stegeman, G.J. Uijen, J.P. de Weerd, "Solution methods of electrical field problems in physiology", *IEEE Trans. Biomed. Eng.*, vol. 29, pp. 34-42, 1982
16. L.D. Landau, E.M. Lifshitz, *Fluid mechanics*, New York: Pergamon Press, 1975
17. L. Lindstrom, R. Magnusson, "Interpretation of myoelectric power spectra: a model and its applications", *Proc. IEEE*, vol. 65, pp. 653-62, 1977
18. M.M. Lowery, N.S. Stoykov, A. Taflove, T.A. Kuiken, "A multiple-layer finite-element model of the surface EMG signal", *IEEE Trans Biomed Eng*, vol. 49, pp. 446-54, 2002
19. M.M. Lowery, N.S. Stoykov, T.A. Kuiken, "A simulation study to examine the use of cross-correlation as an estimate of surface EMG cross talk", *J Appl Physiol.*, vol. 94, pp. 1324-34, 2003
20. R. Merletti, L. Lo Conte, E. Avignone, P. Guglielminotti, "Modeling of surface myoelectric signals--Part I: Model implementation", *IEEE Trans Biomed Eng.*, vol. 46, pp. 810-20, 1999
21. L. Mesin, D. Farina, "Simulation of surface EMG signals generated by muscle tissues with inhomogeneity due to fiber pinnation", *IEEE Trans. Biomed. Eng*., in press
22. R. Plonsey, "Action potential sources and their volume conductor fileds*", IEEE Trans. on Biomed. Eng.*, vol. 56, pp. 601-611, 1977

23. R. Plonsey, R.C. Barr , *Bioelectricity: A Quantitative Approach*, Plenum Pr , 2000

24. H. Reucher , G. Rau , J. Silny, “Spatial filtering of noninvasive multielectrode EMG: Part I--Introduction to measuring technique and applications”, *IEEE Trans Biomed Eng*. , vol. 34, pp. 98-105, 1987

25. H. Reucher, J. Silny, G. Rau, “Spatial filtering of noninvasive multielectrode EMG: Part II--Filter performance in theory and modeling”, *IEEE Trans Biomed Eng.*, vol. 34, pp. 106-13, 1987

26. J. Schneider, J. Silny, G. Rau, “Influence of tissue inhomogeneities on noninvasive muscle fiber conduction velocity measurements--investigated by physical and numerical modeling”, *IEEE Trans Biomed Eng.*, vol. 38, pp. 851-60, 1991

27. I. Sneddon, *Mixed Boundary Value Problems in Potential Theory*, Amsterdam, The Netherlands: North-Holland, 1966

28. D.F. Stegeman, J.H. Blok, H.J. Hermens, K. Roeleveld, “Surface EMG models: properties and applications”, *J Electromyogr Kinesiol.*, vol. 10, pp. 313-26, 2000

29. P.R. Wallace, *Mathematical Analysis of Physical Problems*, Dover, 1984

30. S. Xiao, K. G. McGill, V. R Hentz. “Action potentials of curved nerves in finite limbs”, *IEEE Trans Biomed Eng.,* vol. 42, pp. 599-607, 1995

31. W. Yao, R.J. Fuglevand, R.M. Enoka. “Motor-unit synchronization increases EMG amplitude and decreases force steadiness of simulated contractions”, *J Neurophysiol*., vol. 83, pp. 441-52, 2000

Figure captions

Fig. 1 Effect of an inhomogeneity on the surface potential generated in a homogeneous volume conductor. a) The impulse response is perturbed by a term which is not space invariant, and whose support propagates in the inverse direction with respect of the source. b) The potential along the direction $\vec{s} = \vec{r}_p - \vec{r}_s$, given by the approximate solution of Eq. (9), with $\vec{A} \cdot \vec{n}$ defined by Eq. (11); the perturbation effect decays rapidly with distance from the inhomogeneity. c) Contour plot of the perturbation term for different positions of the impulsive source.

Fig. 2 Analysis of the approximation error in the direction orthogonal to $\vec{r}_p - \vec{r}_s$. The perturbation term should vanish where the normal derivative of the inhomogeneity free potential to the inhomogeneity boundary vanishes. Such a property is verified in a plane orthogonal to $\vec{r}_p - \vec{r}_s$ passing through the tangent points of the lines through the source to the inhomogeneity surface. The approximated perturbation term vanishes in the plane orthogonal to $\vec{r}_p - \vec{r}_s$ passing through the center of the inhomogeneity. In the case of the source in position 1, the distance between the two planes is negligible with respect to the radius of the inhomogeneity.

Fig. 3 Approximated potential along the direction $\vec{s} = \vec{r}_p - \vec{r}_s$ (Eq. (9), (11)). Examples of perturbation terms for different conductivities of the inhomogeneity. a) $\sigma_p = +\infty$, b) $\sigma_p = 0$; in the first case, the values of the potential should be equal at the inhomogeneity boundary (i.e., at s_p-R and s_p+R), in the second, the normal derivative of the potential (i.e., $\frac{d\varphi}{ds}$) should vanish. c), d) intermediate cases; in the first case, the ratio between the conductivity of the inhomogeneity and of the outer volume conductor is larger than unity, in the second it is smaller. In the first case the difference between the potential in s_p-R and s_p+R with respect to the inhomogeneity free potential is reduced, in the second case it is enhanced, whereas the normal derivative is reduced in magnitude. A.U. stands for arbitrary units.

Fig. 4 Effect of the perturbation term relative to an inhomogeneity over the potential detected at another inhomogeneity. a) Definition of the terms in Eq. (17). The quantities are normalized with respect to the inhomogeneity radius *R*. b) Source and inhomogeneities aligned. The dimensions in a) are maintained. $(d^{wc})_{12}$ is the worst case value for *d* in Eq. (17), which is obtained in the aligned situation. Furthermore the effect of an inhomogeneity on the potential over the second is enhanced in the aligned case. c) Schematic representation of the surface potential. The superposition of the effects of the two inhomogeneities is underlined. d) Image theorem for a planar volume conductor. Two inhomogeneities are to be considered even if the volume conductor under consideration contains only one.

Fig. 5 Two layer planar volume conductor constituted by an isotropic fat layer and an anisotropic muscle tissue. The notations of Eq. (21) and subsequent are reported.

Fig. 6 Example of surface EMG signals filtered by different spatial filters (monopolar, longitudinal single and double differential, normal double differential, b)) in the case of absence and presence of a spherical inhomogeneity ($\sigma_p = 10\sigma$). Two positions of the inhomogeneity are considered: aligned with the source and the detection point, and displaced by 2.5 mm, a). A section perpendicular to the fiber of the volume conductor is shown in a). The simulated signals are shown in c) (conduction velocity 4 m/s, tripole model of the source, with parameters from [20]). The muscle fiber was assumed of infinite length. The conductivity values are $\sigma = 0.02$ S/m, $\sigma_{MT} = 0.1$ S/m, $\sigma_{ML} = 0.5$ S/m. Different spatial filters present different sensitivities to local inhomogeneities.

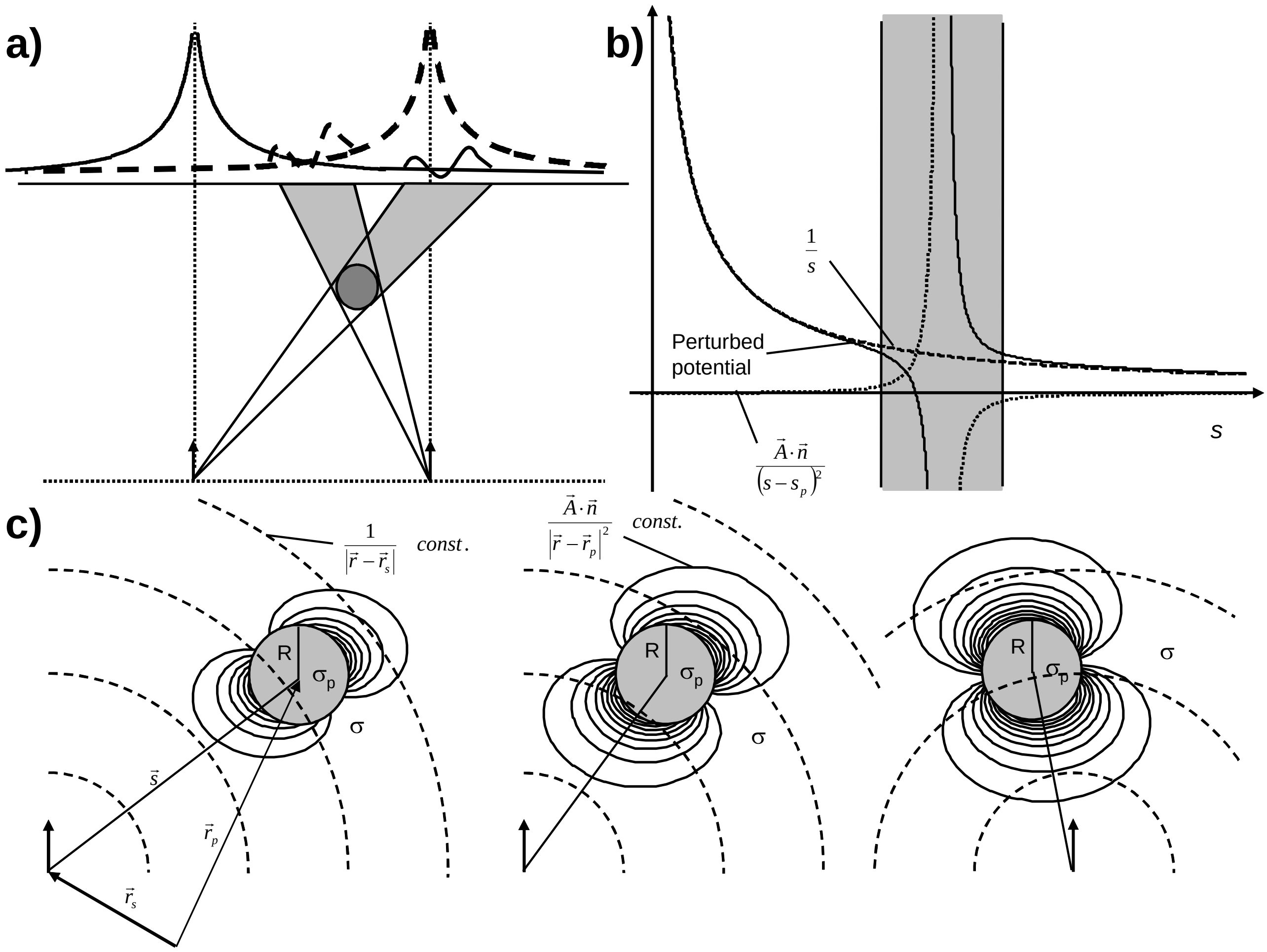
a)
b)
1/s
Perturbed potential
$\frac{\vec{A}\cdot\vec{n}}{(s-s_p)^2}$
s
c)
$\frac{1}{|\vec{r}-\vec{r}_s|}$ const.
$\frac{\vec{A}\cdot\vec{n}}{|\vec{r}-\vec{r}_p|^2}$ const.
R
σ_p
σ
$\vec{s}$
$\vec{r}_p$
$\vec{r}_s$

Figure 1

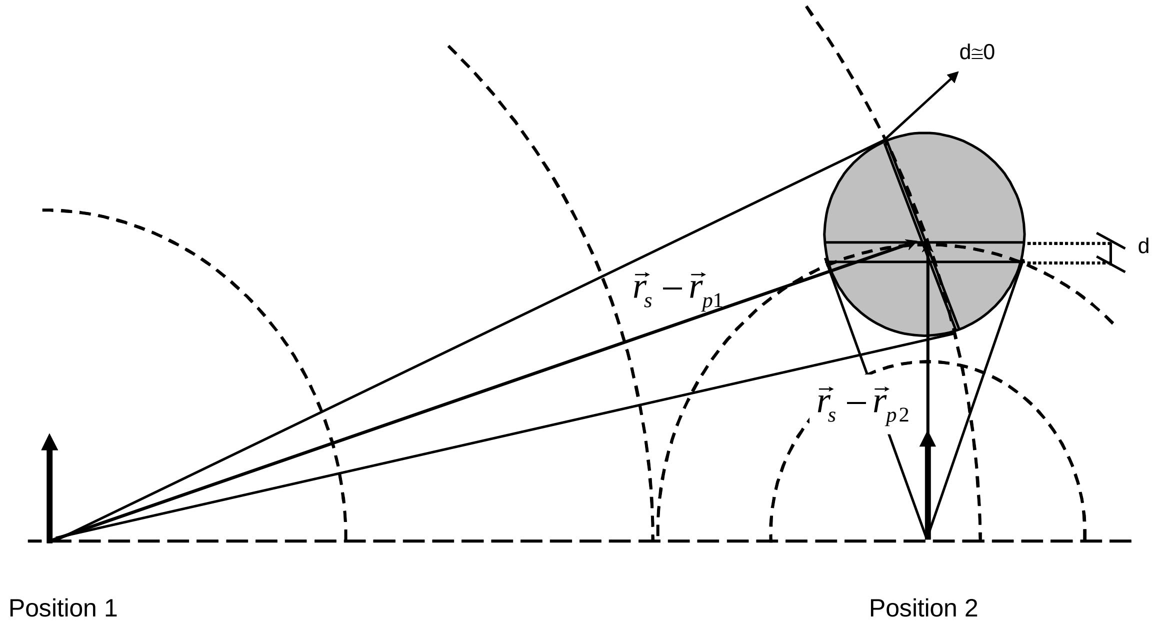

Figure 2

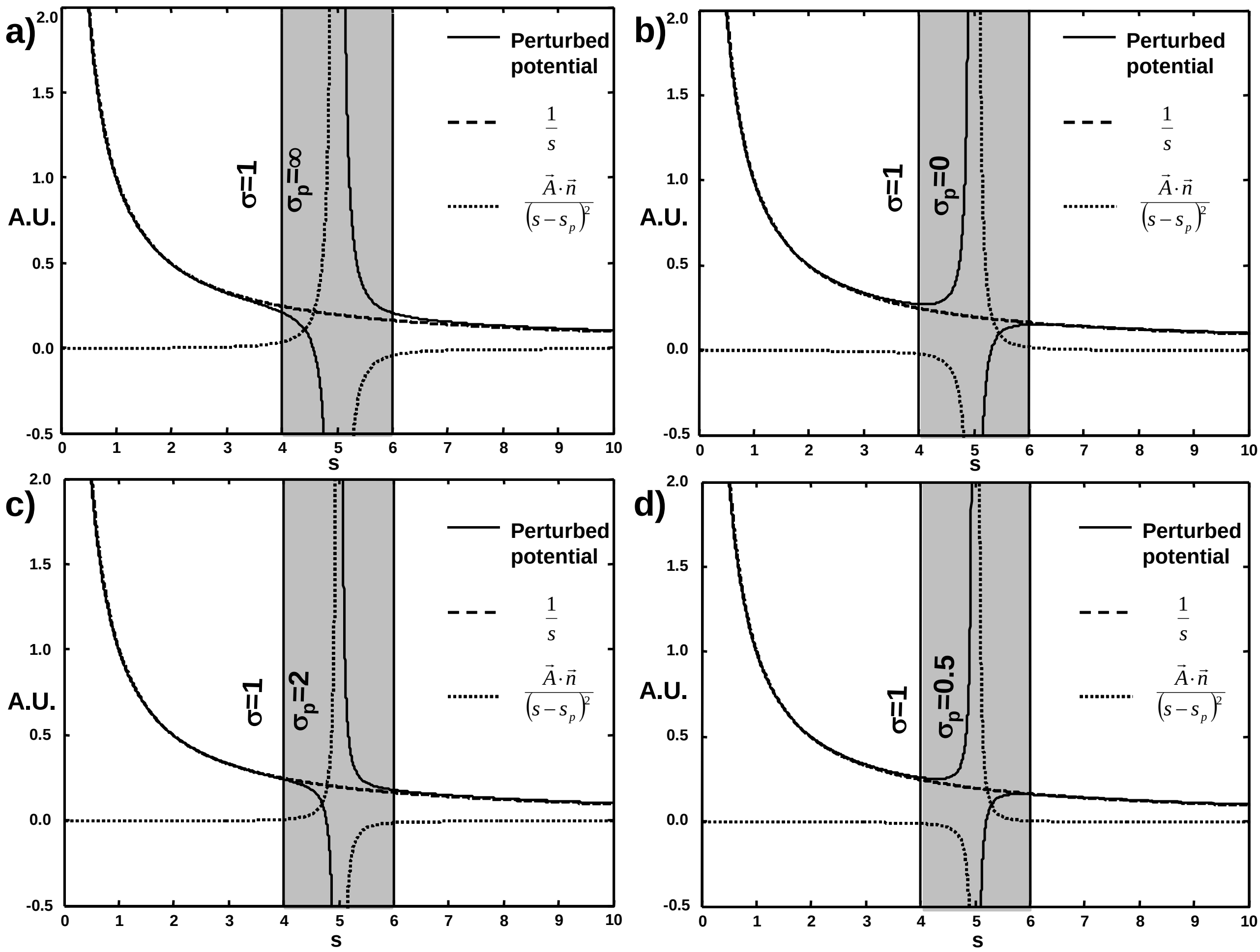
a)
b)
c)
d)
Perturbed potential
$\frac{1}{s}$
$\frac{\vec{A}\cdot\vec{n}}{(s-s_p)^2}$
σ=1
$\sigma_p=\infty$
$\sigma_p=0$
$\sigma_p=2$
$\sigma_p=0.5$
A.U.
s

Figure 3

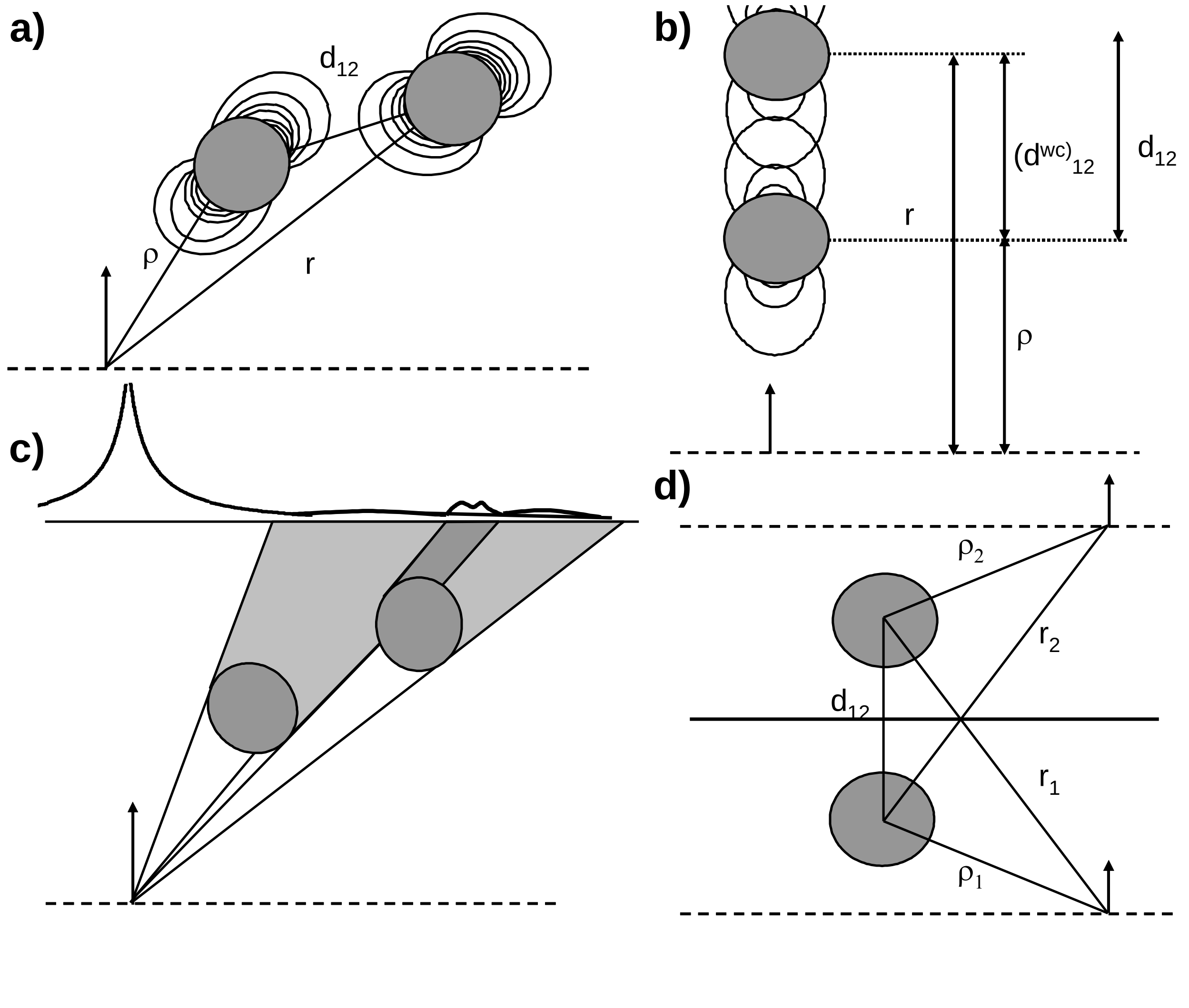

Figure 4

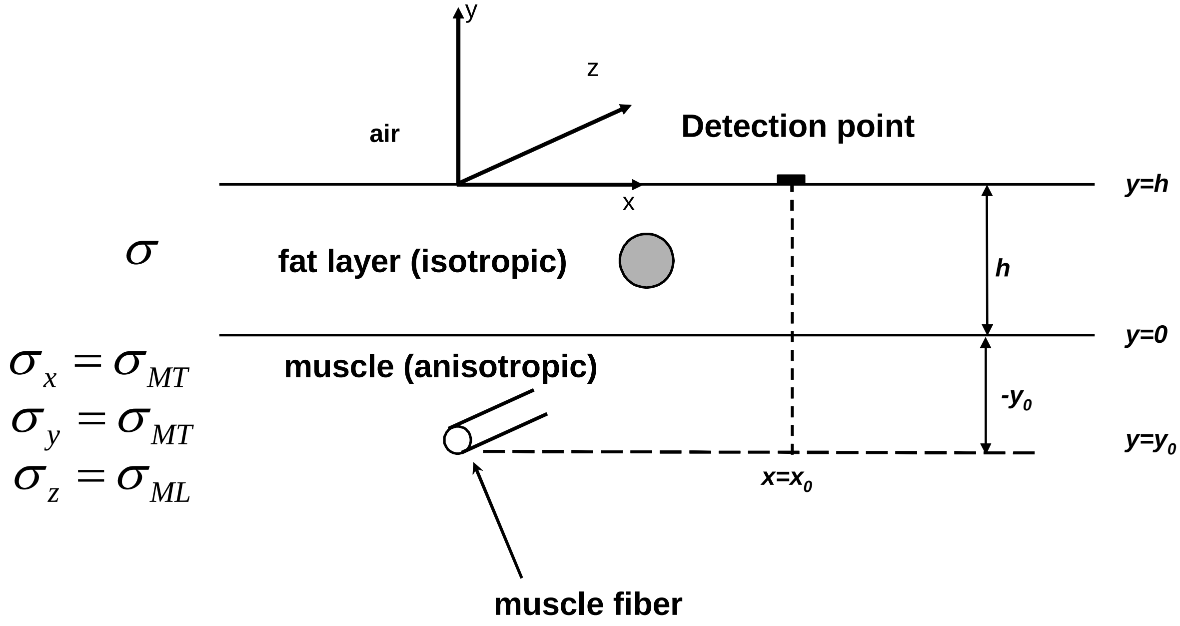

y
z
air
Detection point
x
y=h
σ
fat layer (isotropic)
h
y=0
$\sigma_x = \sigma_{MT}$
$\sigma_y = \sigma_{MT}$
$\sigma_z = \sigma_{ML}$
muscle (anisotropic)
$-y_0$
$y=y_0$
$x=x_0$
muscle fiber

Figure 5

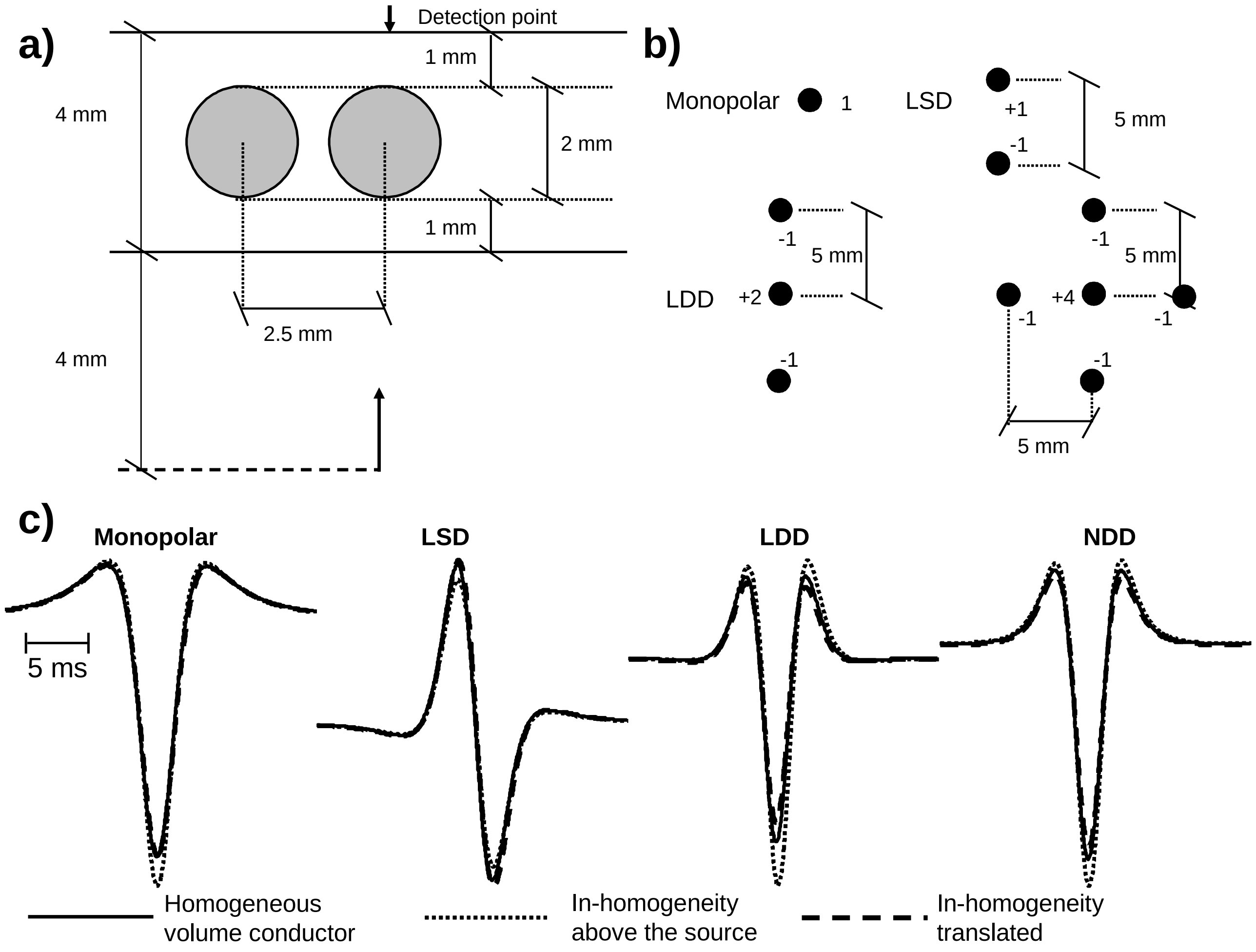

a)
Detection point
1 mm
4 mm
2 mm
1 mm
2.5 mm
4 mm
b)
Monopolar
1
LSD
+1
-1
5 mm
-1
5 mm
LDD
+2
-1
-1
5 mm
+4
-1
-1
-1
-1
5 mm
c)
Monopolar
LSD
LDD
NDD
5 ms
Homogeneous volume conductor
In-homogeneity above the source
In-homogeneity translated

Figure 6